Materials Today Chemistry 28 (2023) 101368

Contents lists available at ScienceDirect

Materials Today Chemistry

journal homepage: www.journals.elsevier.com/materials-today-chemistry/

Studying Na criticality in $Na_xMn_{2-x}O_2$ (x = 1.05–1.3) type Na-rich disordered rocksalt cathode for higher capacity

Bala Krishnan Ganesan [a], Ranjith Thangavel [b, **], Yun Sung Lee [a, *]

[a] School of Chemical Engineering, Chonnam National University, Gwangju 61186, Republic of Korea
[b] School of Energy Science and Engineering, Indian Institute of Technology Guwahati, Guwahati 781039, India

ARTICLE INFO

Article history:
Received 19 August 2022
Received in revised form
16 November 2022
Accepted 26 December 2022
Available online 25 January 2023

Keywords:
Sodium-rich cathode
Montecarlo simulation
Sodium percolation
Sodium diffusion

ABSTRACT

Disordered rocksalt (DRX) can achieve far better capacity than layered oxide cathodes, with the potential to use as cathodes for next-generation batteries, but are limited by their poor ion diffusion kinetics. Initial assessments on Li-rich disordered cathode suggest that Li percolation is heavily influenced by transition metal (TM) polyhedral surrounding Li diffusion path by a repulsive force. However, the kinetics and influence of TM polyhedral structures are not investigated for sodium rich DRX cathodes. Herein, we study the influence of Na stoichiometry in Na-rich DRX cathode—$Na_xMn_{2-x}O_2$ (x = 1.05–1.3) and its influence on Na percolation. Increasing the Na stoichiometry systematically gives better insight into Na percolation network, TM cluster formation, and its effect on sodium diffusivity on Na-DRX cathodes. The cathode material is analyzed by transmission electron microscopy and X-ray absorption spectroscopy analysis, giving better understanding on influence of Na stoichiometry on its neighboring polyhedral structures. The Na-rich samples were initially assessed by electrochemical studies, which showed about 110 $mAhg^{-1}$ of capacity for 0.5 Ag^{-1} current density. The study provides an insight into crystal structure of Na-rich disordered cathode and ways to improve its capacity and rate performance.

© 2022 Elsevier Ltd. All rights reserved.

1. Introduction

With sodium ion being best alternative to replace lithium-based batteries due to their high cost and low availability, sodium is highly limited by its capacity bottlenecks. Due to larger ionic size than lithium, sodium analogs need lot of attention for its betterment toward stationery energy storage application. Recently, many approaches are being made in rocksalt cathodes by converting them into disordered rocksalt (DRX) to improve its capacity and rate performance [1–3]. With much better capacity and rate performance, these DRX materials are well capable as next generation battery cathode due to their low cost and abundant availability. Especially, Ceder et al. group is working on this type of materials that are lithium excess in content with great initial capacity but poor cycle stability [2,4–10]. This emphasis the fact that in addition to cation (Li or Na) excess condition, some parameters or guidelines must be made available to achieve maximum performance. These improvements are made by trial and error with limited or without any parameter guidelines.

Until recently, many rocksalt compounds of sodium ion have been explored greatly. Among these various positive electrodes, Na_xTmO_2 cathodes (Tm – transition metals) are very promising owing to their high conductivity, better performance, and superior cycle stability [11–14]. Most such rocksalt cathodes are analogs of their cathodes for lithium-ion battery system. The most common type of cathodes are O3 [12,15]and P2 [14,16–18], which represents octahedral and prismatic coordination of sodium with three and two layers of TM slabs in a layered rocksalt cathode. Until recently, it is believed that more the structure is layered, more the performance is achieved. This fact remained valid as facile diffusion of sodium was enabled by highly layered structures. During this diffusion process, the sodium ions were largely diffusing through hopping mechanism from one octahedral site to next via tetrahedral sites in-between. Such a hopping mechanism causes lot of disturbance in adjacent TmO_2 layer leading to sliding of same and increasing energy barrier for hopping. Cumulatively, such a series of events lead to capacity loss with increase in cycle. Also, they are

* Corresponding author.
** Corresponding author.
E-mail addresses: ranjith.t@iitg.ac.in (R. Thangavel), leeys@chonnam.ac.kr (Y.S. Lee).

https://doi.org/10.1016/j.mtchem.2022.101368
2468-5194/© 2022 Elsevier Ltd. All rights reserved.

capped by a glass ceiling of capacity of about 120 mAh/g, which needs to be improved drastically to make them fit for commercial applications as mentioned above.

To overcome this capacity limitation, an alternative set of cathodes that are cation (Li or Na) rich are currently being studied. The main advantage of these being number of cation available per unit formula (Li, Na >1) of cathode being much higher than in layered rocksalt cathodes [1,19–22]. Various theoretical studies on enhanced performance of these cation-rich cathodes attributes to "0-TM channels" especially in the case of Li cathode [5,7]. Lee et al. [3] found that when Li diffusion occurs inside cathode structure, they migrate between octahedral sites via tetrahedral channels adjacent to them; however, during this diffusion, significant repulsive forces were exerted by TM containing tetrahedral clusters to activated Li^+ in tetrahedral site. This activated Li^+ becomes more confined inside these tetrahedral sites with increase in Tm-tetrahedral clusters and leads to more restricted diffusion. By demonstrating five different types of clusters namely 0-TM to 4-TM, 0-TM, and 1-TM was found to highly favorable for activated Li^+ diffusion from tetrahedral site to nnn octahedral site by exerting minimum repulsion through "0-TM channel". During Li diffusion process, in contrast to hopping mechanism in above layered structures, the Li diffuses through a percolating network of Li-coordinated sites. Additionally in DRX, short range order (SRO) also determines the lithium diffusivity, which is very much altered by cation (lithium) content [3,23]. In SRO, a small cluster of cathode ion and oxygen may position themselves together to form a ordered layered domain inside random disordered structure. The more occurrence of SRO reduces the occurrence of Li_4 tetrahedra, which in turn leads to reduction 0-Tm Li percolation. Although this SRO is statistically studied using Monte–Carlo simulations and DFT studies [5,10,24], these studies are mostly limited to lithium metal than sodium. During Monte–Carlo simulations, it was evident that Li percolation significantly reduced when the SRO increased by obstructing the lithium diffusion pathways. Hence, reduction in SRO is mandatory for achieving superior capacity and rate performance.

Although all these studies were made using Li as cation, so for not many studies have been conducted on sodium counterparts, which are similar in behavior like lithium but bigger in size and more abundant [20,25–30]. Among them, study on effect of Fe^{3+} for Ru^{4+} by Siriwardena et al. is one of the earliest report on $Na_xMn_{2-x}O_2$ (x = 1.05–1.3) type cathode material. Owing to great demand for sodium-ion as a replacement of Lithium-ion, to the best our knowledge, there have been no previous reports on DRX type Na_xMnO_2 so far. Although Na also follow similar diffusion mechanism as Li, owing to their bulkier size, diffusion kinetics may change and hence the performance. Hence, this knowledge gap on Na-rich DRX should be addressed effectively. Also, the critical Na cation concentration above which 0-TM percolation is much likely possible can give many researchers an option to decide on stoichiometry to synthesize for better capacity and stability.

This knowledge gap motivated us to develop a strategy based on statistical calculation and further apply them in real-time experimental conditions. In this article, we used Monte-Carlo simulation as a statistical tool to analyze the best sodium-rich stoichiometry including predicting its structural behavior. Further predicted structures were systematically analyzed using relevant experimental synthesis and validated for each case to case. To achieve robustness to our findings, real-time problems such as cation-mixing were also included as parameter in Monte–Carlo simulation. To address the stability issues, Na-excess samples were further analyzed by relevant electrochemical and X-ray-based techniques to gain better insights into their valency and its corresponding effect in oxygen atoms.

2. Experimental procedure

2.1. . synthesis of DRX-$Na_{1+X}Mn_{1-X}O_2$ (B-NMO)

B-NMO was synthesized using a conventional solid-state method and successive ball-milling technique to induce disorder. Stoichiometric amounts of Na_2CO_3 (Sigma Aldrich, >99.5%), manganese (III) oxide (Sigma Aldrich, 99%), and 20 wt% citric acid (Sigma Aldrich, 99%) were milled for 6 h using acetone as solvent. Later, the milled precursors were dried in vacuum oven and pressed into pellets. Samples were heated to 700 °C for 12 h at a heating rate of 5 °C/min in a muffle furnace and quenched to room temperature in vacuum atmosphere of glovebox's chamber to yield NMO. To avoid contact with air and moisture, the samples were stored inside glovebox for future progress. The samples were later ball milled in inert atmosphere without any solvent for 36 h at 500 rpm. After ball milling, dark powdered samples namely BNMO-1.05, BNMO-1.1, BNMO-1.2, and BNMO-1.3 expecting sodium stoichiometry of Na-1.0, Na-1.1, Na1.2, and Na-1.3, respectively.

2.2. Material characterization

Crystal structures were characterized by X-ray diffraction (XRD; Cu Ka radiation, Rint 1000, Rigaku, Japan) in 2Θ range of 5–90°. The particle morphology, elemental composition, and internal structure were evaluated using field emission scanning electron microscopy (FE-SEM, S-4700, Hitachi, Japan) coupled with an energy-dispersive X-ray spectroscopy (EDX) module, and high-resolution transmission electron microscopy (HR-TEM; JEM-2000, EX-II, JEOL, Japan).

2.3. Electrochemical measurements

The electrochemical studies of all samples were performed using CR2032 coin cells assembled inside a glovebox under a controlled atmosphere of ultrapure argon. The cells consisted of the synthesized material as the cathode and metallic Na as the anode separated by a polypropylene separator, with 1 M NaClO4 in a mixture of ethylene carbonate (EC) and diethyl carbonate (DEC) (1: 1, v/v) as the electrolyte. The cathode materials were prepared by mixing 5.0 mg of active material with 1.0 mg of Ketjen black and 1.0 mg of teflonized acetylene black (TAB-2). The obtained mixtures were pressed on stainless steel current collector and dried in an oven at 160°c for 4 h before cell fabrication. Charge–discharge (C–DC) studies were performed for different voltage ranges at current rates varying from 0.05 to 1 A/g using a Wonatek WBCS 3000 battery test system. Cyclic voltammetry and EIS analyses were conducted using an electrochemical analyzer (SP-150, Biologic, France).

3. Result and discussions

3.1. X-ray diffraction analysis

To determine the crystal structure, XRD analysis was performed on all samples from 10 to 90°. In Fig. 1, the broader peaks represent the size reduction of particles due to high-intensity ball milling. The peak intensities were very weak due to intense ball milling irrespective of increase in Na stoichiometry from 1.05 to 1.3. Such reduction in XRD peak intensity after ball milling is in good agreement with earlier report by Yabuuchi et al. group [31]. Ball milling time is optimized for 36 h in which maximum particle size

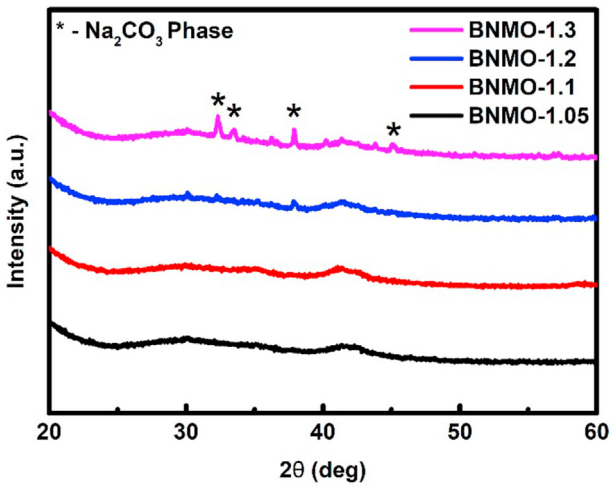

Fig. 1. X-ray diffraction images of disordered rocksalt sodium cathode with increase in Na content.

reduction and disorderness is induced. It is to be noted that ball milling time was optimized based another cathode material with same $NaMnO_2$ and F-doping as shown in Fig. S1. A broad peak at about 42.6° corresponds to high intensity peak of $NaMnO_2$ layered structure corresponding to (1 1 1) plane. With increase in sodium, an additional minor peak is represented in Fig. 1 as *, which corresponds to excess sodium carbonate that readily reacts with outer atmosphere to form sodium carbonate analogs when exposed. Since all our samples were characterized with Kepton tape seal, such exposure to external atmosphere was significantly reduced. With inducing disorderness in rocksalt cathode, the possibility of 0-Tm is drastically increased, which is discussed in the coming sections.

3.2. Electron microscopy

To analyze the microstructure and changes in morphology, electron microscopy images were taken and analyzed. In scanning electron microscopy (SEM), the particles were observed to be coarse in nature with few agglomerates throughout. Further the samples were analyzed using TEM for both imaging and SAED pattern. As shown in Fig. S2, in SAED pattern, the amorphous nature of disordered cathode was confirmed by concentric circle formation. SRO is a common phenomenon observed in cation-rich electrode samples (esp. Li-rich electrodes). To visualize the same, TEM can be an effective tool to observe such SRO. In our samples from BNMO − 1.05–1.2 with increase in Na stoichiometry, the SRO was visibly reduced as encircled in Fig. 2. Since SRO is directly related with 0-Tm percolation, decrease in SRO may result in increase in capacity which is discussed in coming sections. In addition to SRO, amorphous feature was prominent throughout the electrode. In summary, from electron microscopy, it is evident that SRO has reduced significantly with increase in sodium content.

3.3. Electrochemical analysis

To evaluate the electrochemical performance of these samples, they were tested using galvanostatic charge–discharge (GCD), rate performance, cycle stability followed by dQ/dV curve. In GCD at 50 mA/g, among all samples, BNMO-1.1 delivered the highest initial capacity of 165 mAh/g, followed by BNMO-1.2 giving 159 mAh/g. In Fig. 3A, it is to be noted that initial charging capacity was consistently increasing with increase in Na content. Although GCD of

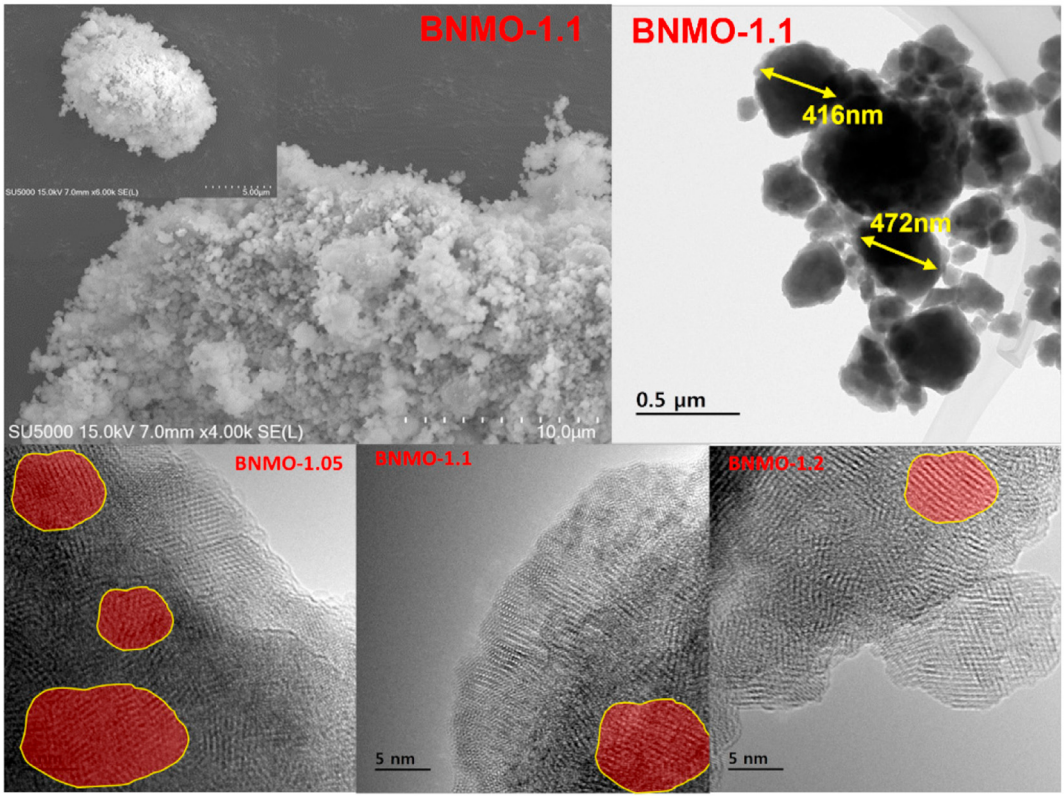

Fig. 2. Electron microscopy images of Na-rich disordered rocksalt cathodes; encircled areas highlight the short range order (SRO).

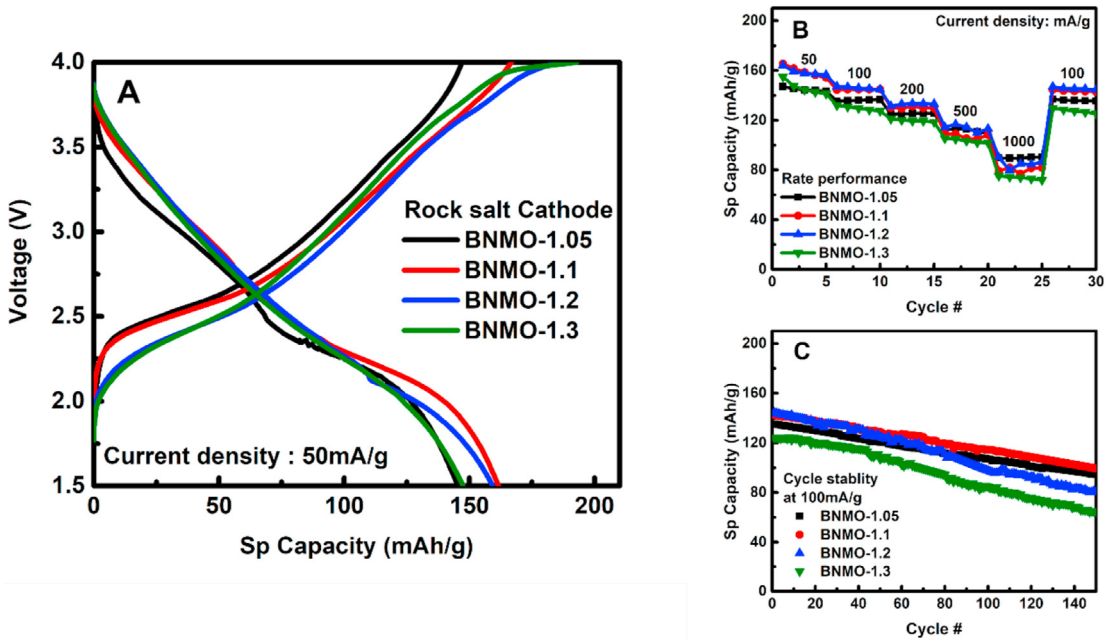

Fig. 3. Galvanostatic charge–discharge of Na-rich cathode materials (A); rate performance at different current density (B); cycle stability at 100 mA/g current density.

$NaMnO_2$ is typically stepwise in nature, in our case, after the formation of disordered structure, the curve became smooth much like capacitive behavior. The smooth charge–discharge behavior could be attributed to smooth sodium ion diffusion three dimensionally through the disordered crystal structure. As seen in earlier reports of Li counterparts with Mn as TM, a smooth discharge curve with a subtle plateau near 2.2 V demonstrates facile and additional Na extraction from crystal structure in comparison to our earlier report of layered [10,32,33]. An improvement both in capacity and in subsequent cycles was achieved by induced disorderness by ball milling. Such a facile Na diffusion is reflected in rate performance too. As shown in Fig. 3B, with increase in current density from 0.05 A/g to 1 A/g, the capacity dropped from 165 to 81 mAh/g of capacity, respectively, for BNMO-1.1. Owing to additional Na percolation pathway enabled by excess Na, such minimal loss in capacity is very much in agreement with improved sodium conductivity in disordered crystal structure.

To evaluate the structural integrity, the samples were cycled at 0.1 A/g. In Fig. 3C, upon cycling, the BNMO-1.1 could display capacity retention of about 81% after first 100 cycles. Although the capacity fade is not on par to that of many sodium layered cathodes, however, the capacity face is much lesser than their Li counterparts [34–37]. Such a capacity fade is mainly associated with spinel formation Li/Na-based electrodes. On the other side, layered electrode materials display great structural stability due to reinforcement support given by Tm layers, which remains intact when Na undergoes electrochemical conversion during cycling. Unfortunately, when the Na content is increased, the Tm content is reduced correspondingly and so do reinforcement pillar of these cathodes is reduced correspondingly.

3.4. Percolation probability analysis

To further understand this improved capacity, rate performance and cycle stability of disordered structure which evolved from layered structure, a 10 × 10 × 10 structure model was generated, and subsequent percolation studies were done by Monte–Carlo simulation based on those models. In constructing the model based on model proposed by Cooper et al. [38], two type of polyhedral were considered namely Na -polyhedra (colored box) and Tm-polyhedra (white box). The model was constructed in such a way that each polyhedral is constructed randomly and limited only by chemical composition (x). Adding to that, cation mixing (i.e. number of Tm in Na-layer/number of Tm in Tm-layer) is also added as cation mixing is one critical factor that greatly influences percolation property of any electrode material. In this model, when two or more polyhedral combine together, they form a cluster, and when these clusters are connected for bottom to top (layer 1 to 10), the system is assumed to be percolating. Although 2D Na conduction along same Na layers is more common among layered electrodes, in our model, the percolation Na ion between two layers of Na is predicted using our model. Such connectivity among layers translates to an alternative sodium diffusion pathway and rate performance in macroscopic level.

Initially by emulating the theoretically ideal states of layered to sodium-rich rocksalt structure, the cation mixing fraction was kept at 0 and corresponding structure was generated in Fig. 4. In a given instance, it can be noted that colored cells correspond to Na polyhedra at different layer, whereas the white cells correspond to Tm octahedra. When Na fraction was increased from 0.8 to 1.0, Na percolation channel remains closed until composition ‘x’ reaches 1.0 and opens beyond. The junction between 1.0 and 1.2 is critical below which the probability of 0-Tm percolation doesn't happen and above which the probability of percolation is maximum (near 1). To estimate this percolation probability in real case, we included cation mixing fraction as another factor added to Na composition. With increase in mixing fraction, chances are that straight line Na percolation channel is broken and the network has to find other ways to percolate. In such case, with the increase in cation mixing fraction from 0.0 to 1.0, the corresponding probability of percolation is given in Fig. 5A. Based on 1000 trails for each Na fraction and Cation mixing combination, the gap of transition from percolation minima to maxima widens with increase in cation mixing, whereas the probability of percolation tends to move toward higher value for even lower Na fractions provided cation mixing is near maximum.

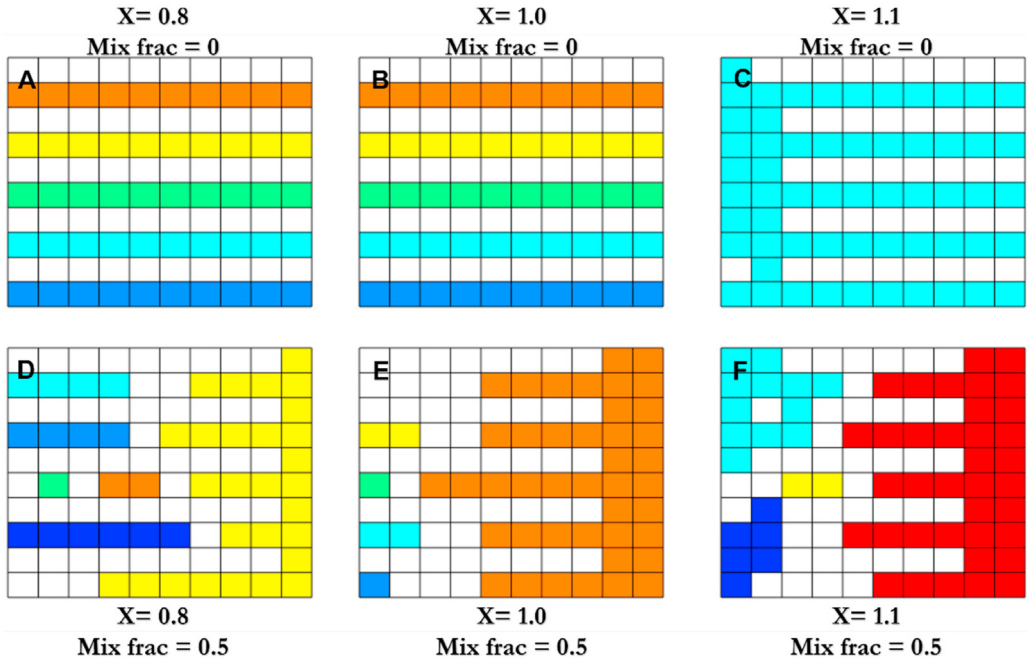

Fig. 4. Na percolation and cluster formation in a 10 × 10 crystal structure with Na polyhedra (colored) and Tm polyhedra (white).

In real cases, the cation mixing can hover somewhere between 0.3 and 0.7, which is entirely dependent on Tm used. In case of Na-deficient ($x \leq 1.0$) cathodes, though these cation mixings can improve Na percolation through one layer to other but in reality, these Na have to travel in 2D direction on a single layer rather than percolating through Tm layer. Such a percolation, indeed, degrades the capacity and performance overall. On the other hand for Na-rich case ($x > 1.0$), these percolation channel acts as additional pathways to extract those extra Na and thus increases capacity as well as performance. It is well understood that Na interlayer percolation can be either incremental or detrimental depending upon Na fraction, and its magnitude is clearly emulated in Fig. 5A.

Additionally, the construction of cell and cluster in Fig explains much about cycle stability of Na-rich samples. It is well known that Tm layers are the backbone/host framework in crystal structure that accommodates and release cation during cycling. It is required that these framework cells are well connected to host cations. In Fig. 4A and B, the formation of isolated cluster of Tm octahedra (white cell) is very minimal or near zero for lower cation mixing. With simultaneous increase in Na content and cation mixing, the number of isolated Tm cluster increases. Such an isolated Tm cluster in surface can easily dissolute into electrolyte leading to capacity loss since not much Tm octahedra available for binding cations together. To validate the Mn dissolution, a pinch of BNMO-1.1 and BNMO-1.3 samples were dipped in electrolyte for overnight to observe any color changes due to dissolution. As shown in Fig. S6, after 12 h, BNMO 1.1 electrolyte was clear whereas color changes appeared in BNMO-1.3, indicating Mn dissolution.

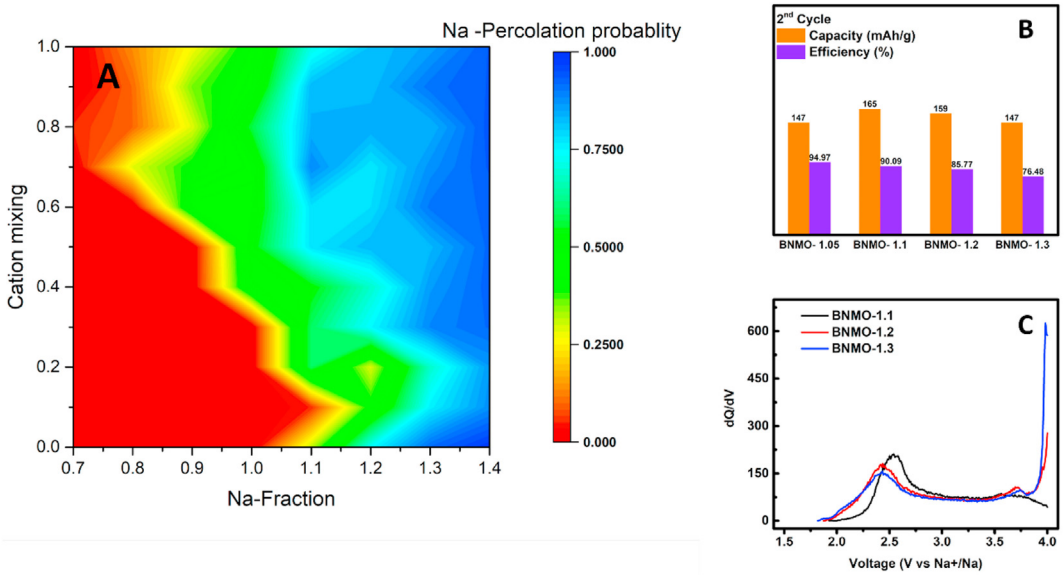

Fig. 5. 0-Tm percolation probability of Na in various $Na_xTm_{2-x}O_2$ structure (A); comparison of capacity and efficiency in various Na cathode (B); dQ/dV curve of charge cycle in various cathodes.

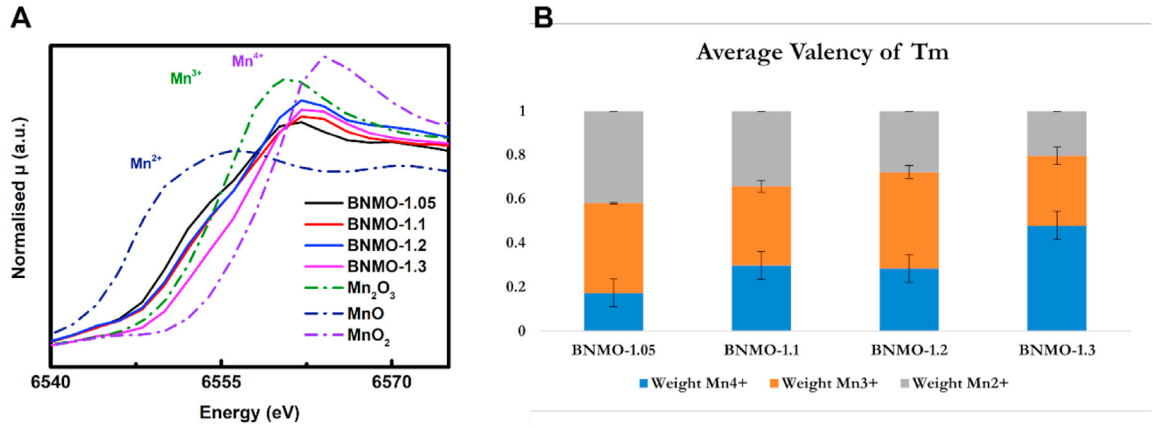

Fig. 6. X-ray absorption near-edge spectra (XANES) of cathode materials in reference to standards (A); valency distribution in cathode material calculated from XANES spectra and linear fitting (B).

To further validate the above theories, the capacity and cycle efficiency of different samples were analyzed in Fig. 5B. It is to be noted that second cycle was considered here rather than first cycle due to fact that in first cycle, majority of cycle efficiency loss happens due to SEI layer formation. Here in second cycle, irrespective of cation mixing, the capacity increased by 12% with increase in Na content from 1.0 to 1.1; upon increasing further, the initial capacity was higher than BNMO-1.05 but decreased with subsequent cycle. This is very much in agreement with our model that with more cycle number, the mixing fraction increases and so do interlayer sodium percolation but compromises intralayer sodium diffusion. On the other side, the cycle stability was also deteriorating aggressively for Na-rich sample in proportion to their Na content due to less availability of Tm cluster and formation of more isolated Tm clusters lost in cycling. Adding to this deterioration, as in Fig. 5C, oxidation may also have contributed in poor cyclability as confirmed by higher dQ/dV at higher potentials for Na-rich samples.

To further investigate the excessive capacity loss in Na-rich samples, the samples were analyzed with XAS analysis in Fig. 6. X-ray absorption near-edge spectra (XANES) is a powerful technique to study the oxidation state of TM used. Since oxidation state is directly linked to capacity and stability of cathode, XANES can be used to analyze the same for any sample. In our samples, when Na content is increased from 1.05 to 1.3, the TM valency also increased from near 3+ to above 3+ for BNMO-1.3 due to reduction in Tm content. Such an increase in valency can result reduced capacity due to nonavailability of +5 oxidation state in Mn and resulting in oxygen loss. Both the capacity loss with increase in Na content beyond critical point and stability loss are in good agreement with increase in Mn valency. Hence it is crucial to evaluate or estimate the exact stoichiometries of cations going into cation-rich electrodes for its overall better performance (see Fig. 7).

In summary, the high-performance Na-rich cathodes are perfect balance between the sodium stoichiometry, structural integrity, and the Tm valency. If the Na stoichiometry is increased, the capacity is drastically increased but the structural stability either due to the cluster formation or Tm valency, the cycle stability is drastically hit. Hence, to improve the same, following remedies can be adopted:

1. Critical sodium-rich content for layered cathode is up to x = 1.3, beyond which impure phases tend to form.
2. Average valency of Tm must be kept as less as possible (i.e., less than 3+) to accommodate additional sodium ion.
3. Alternatively, Tm with wide options in oxidation states (+3 to +6) such as Cr and Mo can be used or anion doping such as F-doping can also be used.

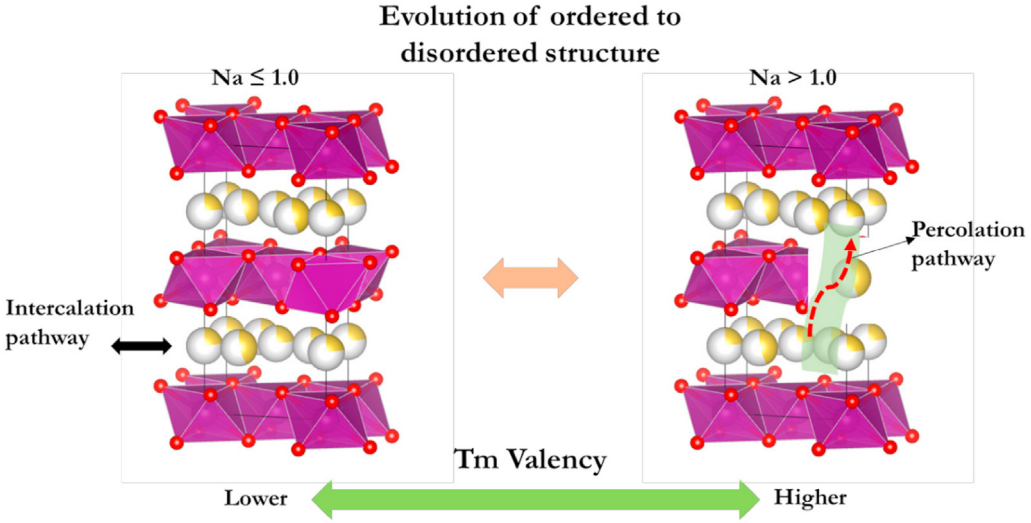

Fig. 7. Schematic representing evolution of cathode structure from Na-deficient to Na-rich and corresponding effect in Tm valency and diffusion pathway.

4. Cation mixing improves both capacity and cycle stability, hence induced cation mixing can be considered as an option.

It is to be noted that abovementioned suggestions are based on our understandings from above studies and requires extensive research to validate the same.

4. Conclusion

Disordered sodium TM oxide rocksalt cathode (DRX) cathodes are class of cathodes whose real potentials are still unexplored. Although poor cycle stability is commonly observed phenomenon, the real root causes, and strategy to improve them are not yet done effectively. In this work, the root cause for improvement in capacity, critical sodium stoichiometry range to achieve the maximum performance are extensively studied both experimentally and using percolation studies by Monte–Carlo simulation. In addition, the reason behind poor cycle performance was studied using simulation of model structure, which gives better insight about structure evolution during sodium addition. The critical sodium content beyond which 3D sodium percolation may happen is much similar to its lithium counterparts that prove validity of these results. However, this study is very preliminary and limited by assumptions such as sodium and TM polyhedral was considered instead of individual atoms that can be done in depth by molecular simulation studies. Overall, this study could be a good starting point for choosing sodium stoichiometry in Na-rich cathode materials and in choosing TMs accordingly for better performance.

Credit author statement

Bala Krishnan Ganesan: Conceptualization, Methodology, Formal analysis, Investigation, Software, Visualization, Writing – original draft. **Ranjith Thangavel**: Methodology, Formal analysis, Investigation, Visualization, Writing – review and editing. **Yun-Sung Lee**: Funding acquisition, Resources, Supervision, Visualization, Validation, Writing – reviewing and editing.

Declaration of competing interest

The authors declare that they have no known competing financial interests or personal relationships that could have appeared to influence the work reported in this paper.

Data availability

Data will be made available on request.

Acknowledgments

This work was supported by the National Research Foundation of Korea (NRF) grant funded by the Korean government (Ministry of Science, ICT & Future Planning) (No.2019R1A2C1007620). Dr. Ranjith Thangavel acknowledges financial support from the Science & Engineering Research Board (SERB), a statutory body of the Department of Science & Technology (DST), Govt. of India, through the Start-up Research Grant (SRG/2022/000642).

Appendix A. Supplementary data

Supplementary data to this article can be found online at https://doi.org/10.1016/j.mtchem.2022.101368.

References

[1] D.P. Siriwardena, J.F.S. Fernando, T. Wang, K.L. Firestein, C. Zhang, J.E. von Treifeldt, D.V. Golberg, Effect of Fe^{3+} for Ru^{4+} substitution in disordered Na1.33Ru0.67O2 cathode for sodium-ion batteries: structural and electrochemical characterizations, Electrochim. Acta 325 (2019), 134926, https://doi.org/10.1016/j.electacta.2019.134926.
[2] H. Ji, A. Urban, D.A. Kitchaev, D.H. Kwon, N. Artrith, C. Ophus, W. Huang, Z. Cai, T. Shi, J.C. Kim, H. Kim, G. Ceder, Hidden structural and chemical order controls lithium transport in cation-disordered oxides for rechargeable batteries, Nat. Commun. 10 (2019) 1–9, https://doi.org/10.1038/s41467-019-08490-w, 1. 10 (2019.
[3] J. Lee, C. Wang, R. Malik, Y. Dong, Y. Huang, D.H. Seo, J. Li, Determining the criticality of Li-excess for disordered-rocksalt Li-ion battery cathodes, Adv. Energy Mater. 11 (2021), https://doi.org/10.1002/AENM.202100204.
[4] A. Urban, J. Lee, G. Ceder, A. Urban, J. Lee, G. Ceder, The configurational space of rocksalt-type oxides for high-capacity lithium battery electrodes, Adv. Energy Mater. 4 (2014), 1400478, https://doi.org/10.1002/AENM.201400478.
[5] R.J. Clément, Z. Lun, G. Ceder, Cation-disordered rocksalt transition metal oxides and oxyfluorides for high energy lithium-ion cathodes, Energy Environ. Sci. 13 (2020) 345–373, https://doi.org/10.1039/C9EE02803J.
[6] J. Lee, A. Urban, X. Li, D. Su, G. Hautier, G. Ceder, Unlocking the potential of cation-disordered oxides for rechargeable lithium batteries, Science (2014) 519–522, https://doi.org/10.1126/SCIENCE.1246432/SUPPL_FILE/LEE.SM.PDF, 1979). 343.
[7] B. Ouyang, N. Artrith, Z. Lun, Z. Jadidi, D.A. Kitchaev, H. Ji, A. Urban, G. Ceder, Effect of fluorination on lithium transport and short-range order in disordered-rocksalt-type lithium-ion battery cathodes, Adv. Energy Mater. 10 (2020), 1903240, https://doi.org/10.1002/AENM.201903240.
[8] Z. Lun, B. Ouyang, D.A. Kitchaev, R.J. Clément, J.K. Papp, M. Balasubramanian, Y. Tian, T. Lei, T. Shi, B.D. McCloskey, J. Lee, G. Ceder, Improved cycling performance of Li-excess cation-disordered cathode materials upon fluorine substitution, Adv. Energy Mater. 9 (2019), 1802959, https://doi.org/10.1002/AENM.201802959.
[9] H. Ji, D.A. Kitchaev, Z. Lun, H. Kim, E. Foley, D.H. Kwon, Y. Tian, M. Balasubramanian, M. Bianchini, Z. Cai, R.J. Clément, J.C. Kim, G. Ceder, Computational investigation and experimental realization of disordered high-capacity Li-ion cathodes based on Ni redox, Chem. Mater. 31 (2019) 2431–2442, https://doi.org/10.1021/ACS.CHEMMATER.8B05096/SUPPL_FILE/CM8B05096_SI_001.PDF.
[10] Z. Lun, B. Ouyang, Z. Cai, R.J. Clément, D.H. Kwon, J. Huang, J.K. Papp, M. Balasubramanian, Y. Tian, B.D. McCloskey, H. Ji, H. Kim, D.A. Kitchaev, G. Ceder, Design principles for high-capacity Mn-based cation-disordered rocksalt cathodes, Chem 6 (2020) 153–168, https://doi.org/10.1016/J.CHEMPR.2019.10.001.
[11] Ti-Substituted NaNi0.5Mn0.5-xTixO2 Cathodes with Reversible O3–P3 Phase Transition for High-Performance Sodium-Ion Batteries, (n.d.). https://onlinelibrary.wiley.com/doi/epdf/10.1002/adma.201700210 (accessed February 21, 2022).
[12] S. Guo, P. Liu, H. Yu, Y. Zhu, M. Chen, M. Ishida, H. Zhou, A layered P2- and O3-type composite as a high-energy cathode for rechargeable sodium-ion batteries, Angew. Chem. 127 (2015) 5992–5997, https://doi.org/10.1002/ANGE.201411788.
[13] R. Fielden, M.N. Obrovac, Investigation of the $NaNi_xMn_{1-x}O_2$ ($0 \leq x \leq 1$) system for Na-ion battery cathode materials, J. Electrochem. Soc. 162 (2015), https://doi.org/10.1149/2.0551503jes. A453–A459.
[14] C. Wang, L. Liu, S. Zhao, Y. Liu, Y. Yang, H. Yu, S. Lee, G.H. Lee, Y.M. Kang, R. Liu, F. Li, J. Chen, Tuning local chemistry of P2 layered-oxide cathode for high energy and long cycles of sodium-ion battery, Nat. Commun. 12 (2021) 1–9, https://doi.org/10.1038/s41467-021-22523-3, 1. 12 (2021.
[15] I. Lee, G. Oh, S. Lee, T.Y. Yu, M.H. Alfaruqi, V. Mathew, B. Sambandam, Y.K. Sun, J.Y. Hwang, J. Kim, Cationic and transition metal co-substitution strategy of O3-type $NaCrO_2$ cathode for high-energy sodium-ion batteries, Energy Storage Mater. 41 (2021) 183–195, https://doi.org/10.1016/J.ENSM.2021.05.046.
[16] R. Berthelot, D. Carlier, C. Delmas, Electrochemical investigation of the P2-$NaxCoO_2$ phase diagram, Nat. Mater. 10 (2011) 74–80, https://doi.org/10.1038/NMAT2920.
[17] Y. Zhu, W. Nie, P. Chen, Y. Zhou, Y. Xu, Li-doping stabilized P2-Li0.2Na1.0Mn0.8O_2 sodium ion cathode with oxygen redox activity, Int. J. Energy Res. 44 (2020) 3253–3259, https://doi.org/10.1002/er.5120.
[18] S. Guo, Y. Sun, J. Yi, K. Zhu, P. Liu, Y. Zhu, G.Z. Zhu, M. Chen, M. Ishida, H. Zhou, Understanding sodium-ion diffusion in layered P2 and P3 oxides via experiments and first-principles calculations: a bridge between crystal structure and electrochemical performance, NPG Asia Mater. 8 (2016) 4, https://doi.org/10.1038/am.2016.53, 8 (2016) e266–e266.
[19] H. Wang, S. Liu, Y. Ren, W. Wang, A. Tang, Ultrathin Na 1.08V $3O_8$ nanosheets - a novel cathode material with superior rate capability and cycling stability for Li-ion batteries, Energy Environ. Sci. 5 (2012) 6173–6179, https://doi.org/10.1039/c2ee03215e.
[20] L. Chen, S. Jin, H. Liu, S. Chen, Y. Dong, Q. Kuang, Y. Zhao, L. Chen, Structural and electrochemical studies of Fe-doped $Na_3Mn_2P_3O_{11}$ cathode materials for sodium-ion batteries, J. Alloys Compd. 821 (2020), 153206, https://doi.org/10.1016/j.jallcom.2019.153206.

[21] S. Liu, X. Cao, Y. Zhang, K. Wang, Q. Su, J. Chen, Q. He, S. Liang, G. Cao, A. Pan, Carbon quantum dot modified $Na_3V_2(PO_4)_2F_3$ as a high-performance cathode material for sodium-ion batteries, J Mater Chem A Mater 8 (2020) 18872–18879, https://doi.org/10.1039/d0ta04307a.

[22] W.J. Li, S.L. Chou, J.Z. Wang, Y.M. Kang, J.L. Wang, Y. Liu, Q.F. Gu, H.K. Liu, S.X. Dou, Facile method to synthesize na-enriched Na1+xFeFe(CN)6 frameworks as cathode with superior electrochemical performance for sodium-ion batteries, Chem. Mater. 27 (2015) 1997–2003, https://doi.org/10.1021/cm504091z.

[23] Y. Fan, W. Zhang, Y. Zhao, Z. Guo, Q. Cai, Fundamental understanding and practical challenges of lithium-rich oxide cathode materials: layered and disordered-rocksalt structure, Energy Storage Mater. 40 (2021) 51–71, https://doi.org/10.1016/J.ENSM.2021.05.005.

[24] J. Lee, A. Urban, X. Li, D. Su, G. Hautier, G. Ceder, Unlocking the potential of cation-disordered oxides for rechargeable lithium batteries, Science 343 (2014) 519–522, https://doi.org/10.1126/SCIENCE.1246432, 1979.

[25] B.K. Ganesan, U.R. Son, R. Thangavel, Y.-S. Lee, Effect of sodium addition on lattice structure and tuning performance in sodium rich $Na_xTm_{2-x}O_2$ type cathode materials (Tm = Mn and Cr; X = 1.05–1.3) - a study, Electrochim. Acta 421 (2022), 140493, https://doi.org/10.1016/J.ELECTACTA.2022.140493.

[26] H.S. Hirsh, Y. Li, D.H. S Tan, M. Zhang, E. Zhao, Y. Shirley Meng, H.S. Hirsh, Y. Li, D.H. S Tan, M. Zhang, E. Zhao, Y.S. Meng, Sodium-ion batteries paving the way for grid energy storage, Adv. Energy Mater. 10 (2020), 2001274, https://doi.org/10.1002/AENM.202001274.

[27] X. Zhang, Y. Qiao, S. Guo, K. Jiang, S. Xu, H. Xu, P. Wang, P. He, H. Zhou, X. Zhang, S. Guo, K. Jiang, S. Xu, H. Xu, P. Wang, P. He, H. Zhou, Y. Qiao, Manganese-based Na-rich materials boost anionic redox in high-performance layered cathodes for sodium-ion batteries, Adv. Mater. 31 (2019), 1807770, https://doi.org/10.1002/ADMA.201807770.

[28] L. Zheng, H. Wang, M. Luo, G. Wang, Z. Wang, C. Ouyang, Na_2MnO_3 as cathode materials for Na ion batteries: from first-principles investigations, Solid State Ionics 320 (2018) 210–214, https://doi.org/10.1016/J.SSI.2018.02.039.

[29] D.P. Siriwardena, J.F.S. Fernando, T. Wang, K.L. Firestein, C. Zhang, J.E. von Treifeldt, D.v. Golberg, Effect of Fe^{3+} for Ru^{4+} substitution in disordered $Na1.33Ru0.67O_2$ cathode for sodium-ion batteries: structural and electrochemical characterizations, Electrochim. Acta 325 (2019), 134926, https://doi.org/10.1016/J.ELECTACTA.2019.134926.

[30] Sci-Hub | Novel structurally-stable Na-rich Na4V2O7 cathode material with high reversible capacity by utilization of anion redox activity. Chem. Commun. | 10.1039/D0CC02816A, (n.d.) (accessed August 19, 2021).

[31] T. Sato, K. Sato, W. Zhao, Y. Kajiya, N. Yabuuchi, Metastable and nanosize cation-disordered rocksalt-type oxides: revisit of stoichiometric LiMnO2 and NaMnO2, J Mater Chem A Mater 6 (2018) 13943–13951, https://doi.org/10.1039/C8TA03667E.

[32] H. Li, R. Fong, M. Woo, H. Ahmed, D.H. Seo, R. Malik, J. Lee, Toward high-energy Mn-based disordered-rocksalt Li-ion cathodes, Joule 6 (2022) 53–91, https://doi.org/10.1016/J.JOULE.2021.11.005.

[33] B.K. Ganesan, U.R. Son, R. Thangavel, Y.S. Lee, Effect of sodium addition on lattice structure and tuning performance in sodium rich $Na_xTm_{2-x}O_2$ type cathode materials (Tm = Mn and Cr; X = 1.05–1.3) - a study, Electrochim. Acta 421 (2022), 140493, https://doi.org/10.1016/J.ELECTACTA.2022.140493.

[34] S.H. Park, S.H. Kang, I. Belharouak, Y.K. Sun, K. Amine, Physical and electrochemical properties of spherical Li1+x(Ni1/3Co1/3Mn1/3)1-xO2 cathode materials, J. Power Sources 177 (2008) 177–183, https://doi.org/10.1016/j.jpowsour.2007.10.062.

[35] S. Song, M. Kotobuki, F. Zheng, Q. Li, C. Xu, Y. Wang, W.D.Z. Li, N. Hu, L. Lu, Na-rich layered Na2Ru0.95Zr0.05O3 cathode material for Na-ion batteries, J. Power Sources 342 (2017) 685–689, https://doi.org/10.1016/j.jpowsour.2016.12.116.

[36] N. Su, Y. Lyu, B. Guo, Electrochemical and in-situ X-ray diffraction studies of Na1.2Ni0.2Mn0.2Ru0.4O2 as a cathode material for sodium-ion batteries, Electrochem. Commun. 87 (2018) 71–75, https://doi.org/10.1016/j.elecom.2017.12.029.

[37] D.P. Siriwardena, J.F.S. Fernando, T. Wang, K.L. Firestein, C. Zhang, J.E. von Treifeldt, D.V. Golberg, Effect of Fe3+ for Ru4+ substitution in disordered Na1.33Ru0.67O2 cathode for sodium-ion batteries: structural and electrochemical characterizations, Electrochim. Acta 325 (2019), 134926, https://doi.org/10.1016/J.ELECTACTA.2019.134926.

[38] percolation theory, (n.d.). https://d-arora.github.io/Doing-Physics-With-Matlab/mpDocs/percolation.htm.